Universidade Federal do Rio Grande do Sul

Study of Thermodynamical Anomalies in Mixtures

Marco Antônio Habitzreuter

Supervised by Prof. Dra.

Marcia Crisina Bernardes Barbosa

Porto Alegre

May, 2021

Abstract

Water-alcohol mixtures can exhibit anomalies in excess quantities. In this work, we attempt to describe these anomalies with a simple model for the water-solute mixture. The system is studied with an exact one-dimensional approach, as well as with three-dimensional simulations. The interactions between particles in the mixture are represented by core-softened potentials and we compute the thermodynamic quantities of interest at constant pressure, temperature, and number of particles. The excess of the temperature of maximum density at small dilutions, the excess of volume, and excess of enthalpy are computed in the one dimensional analysis and in the simulations. The behavior of these quantities is compared with the water-alcohol experimental results.

Contents

List of Figures

1 Introduction

Water is necessary for almost all aspects of our daily lives. This seemingly simple substance is, actually, very interesting, complicated, and with many mysteries yet to be understood, since there are a variety of anomalous behaviors present in water. These anomalies are dynamical and thermodynamical properties in which water behaves differently when compared to most substances. An extensive repository with more than 70 water anomalies has been compiled by Martin Chaplin[1], containing almost 5000 references to scientific papers. For instance, there is an anomalous increase in the isothermal compressibility for a certain range of pressure as the temperature is decreased [1]. Another example is the mobility of water. While most liquids have a lower diffusion coefficient D when compressed, the diffusion of water increases with more pressure, up to a certain point [2, 3]. Water also has a large heat capacity which is fundamental to control variations of temperature in our environment [4]. In clouds, supercooled water influences how radiation is reflected, which impacts our climate [5].

However, one of the most known anomalies is the temperature of maximum density (TMD). At a pressure of 1 atmosphere, above 4 °C water density decreases when heated at constant pressure, just like other substances. But from 0 °C up to 4 °C, the density increases with the increase of temperature. It follows that at 4 °C the density of water is maximum.

Some anomalies can be reproduced with computer simulations using atomistic models to describe water [6–11]. These models select the oxygen and hydrogen distances, angles, and potential interactions to fit specific experimental properties. This technique is quite useful to probe regions of temperatures and pressures that are very difficult to reach experimentally. Atomistic models also take into account many details, making it difficult to separate what is important to explain the anomalies and what is not [12].

In the 70s, core-softened (CS) potentials were introduced, starting with the model proposed by Hemmer and Stell [13, 14]. They have a hard core and an attenuated region, like a ramp or a step as depicted in Figure 1. Instead of representing all hydrogens and oxygens, this coarse-grained potential has two interaction scales: one associated with

[1] lsbu.ac.uk/water

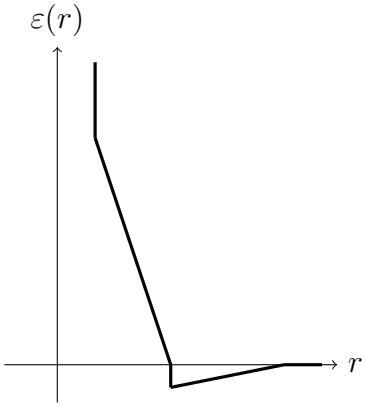

Figure 1: Core-softened (CS) potential used by Hemmer and Stell.

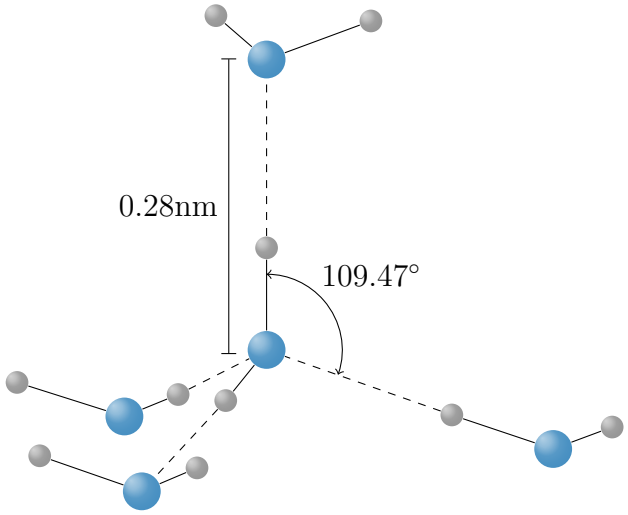

Figure 2: Water with H (dashed) and OH (continuous) bonds. Adapted from [15].

the ramp and another associated with a greater distance, representing the two states of hydrogen bonding in liquid water. These bonds are formed when a hydrogen atom is attracted to an oxygen atom from another water molecule. Each oxygen atom can form two hydrogen bonds and each hydrogen atom can form one. Thus every water molecule can have up to four hydrogen bonds, forming a tetrahedral structure. This is represented in Figure 2.

The core-softened potential displays a region in pressure and temperature with a density anomaly [16] originated from the competition between the two distance scales [12, 17]. From this perspective, the density maximum of water is understood as a result of two opposite effects: decreased density by thermal expansion and increased density by the

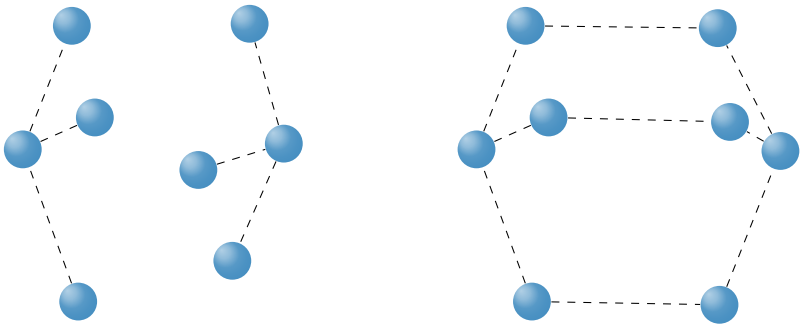

Figure 3: Representation of high (L) and low (R) density structures. Only oxygen atoms are shown. The dashed lines represents the hydrogen bond. Adapted from [20]. The original version has an animated video of this clustering process.

collapse of the tetrahedral structures, as represented in Figure 3. For $T > 4°C$, temperature wins this competition, lowering the density. But in the 0°C to 4°C interval, the effect caused by the disruption of hydrogen bonds in liquid water is the most significant factor: a higher density structure is formed. This interpretation of water anomalies as the competition between two kinds of local structures is also supported by experiments [18, 19].

This potential was also used to simulate other anomalous behaviors such as the diffusion anomaly, structural anomaly, and the isothermal compressibility anomaly [12, 21]. Thus a very simple and computationally inexpensive potential can qualitatively simulate many water anomalies and it's possible second critical point [22, 23].

If water as a pure substance is interesting, in a mixture with other materials it can be fascinating. The temperature of maximum density, for instance, can increase or decrease, depending on the concentration and the type of solute in the mixture, which results from the formed structures [24, 25].

It is common to name alcohols that increase the TMD "structure-makers", in the sense that more temperature is needed to destroy the hydrogen bonds and lower the density, indicating a stronger structure than the pure water tetrahedral structure. Examples of structure-makers include isopropanol, tert-butanol, sec-butanol, 2-butanol [26], ethyl and n-propyl alcohols [27]. The TMD increases up to a certain concentration of solute and then decreases until the anomaly vanishes. On the other hand, solutes that decrease the TMD are called "structure-breaker", such as ethylene glycol, glycerin and phenol [26]. They tend to weaken the hydrogen bond structure, requiring a smaller temperature to

reach the minimum volume.

Another interesting property is the behavior of excess quantities, the difference between a given quantity and the respective value in an ideal mixture. Changes in temperature, pressure and solute in these mixtures generate a very rich behavior. For instance, there is a negative excess enthalpy for methanol [28, 29], with a minimum around 35%. For ethanol, the excess enthalpy changes from negative to positive as a function of increasing temperature [29–31]. For the lower temperature, there is a minimum around 20%, which shifts to a maximum close to 60% for a higher temperature. The excess volume is negative for mixtures with methanol [32], propanol [33], t-butanol [34] and 2-methyl-2-propanol [35]. The excess specific heat is positive for ethanol [31] and tert-butanol [34, 36]. The maximum of c_p^E is also a function of temperature and pressure, ranging approximately from 10 to 30%.

From previous studies that analyzed a one-dimensional system core softened potentials [37, 38], we know that a shoulder-like potential can be used to make useful predictions about three-dimensional systems and to gain intuition about how the system behaves. Inspired by the core-softened potentials which shows a TMD and the surprising effects of water-alcohol mixing, it seems natural to inquire what happens if we apply a similar model to a mixture of particles. Can we see the positive ΔTMD behavior of water-alcohol mixtures with this model? What is the behavior of excess quantities? What is the microscopic mechanism that makes this weird behavior happen?

In the following sections, we explore the thermodynamic behavior of a mixture of particles in one dimension using first a random mixing approximation, followed by an exact solution. By testing several potentials with this exact approach we identify a model which exhibits anomalies in the mixture. Next, we extend this model to three dimensions and compute the excess properties and the change in TMD using Molecular Dynamics simulations.

2 Analytic Solution

Our analysis starts with a general statistical description for one-dimensional binary mixtures inspired by previous studies [39, 40]. We want to find the partition function for an arbitrary potential.

2.1 The Formalism

In order to account for the number of different configurations for two types of particles, A and B, we begin with a discrete model. Consider a line of sites separated by a distance η. Each site could be occupied by a particle or remain empty. Let N_A and N_B represent the number of particles of each type. We denote N the total number of particles and L the total size of the system.

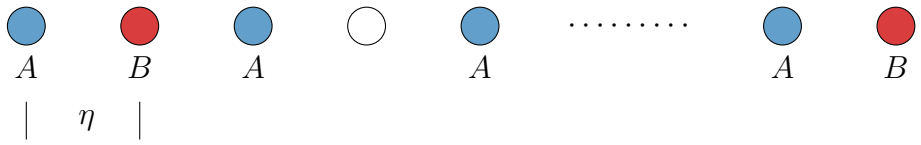

Figure 4: Line of particles

Consider two neighbor particle of type i and j. The distance between them can be expressed with an integer k as $k\eta$. We call $\varepsilon_{ij}^k = \varepsilon_{ij}(k\eta)$ the potential of one over the other. Let ν_{ij}^k be number of first neighbor interactions between particles of types i and j at a distance $k\eta$. From this description, the Hamiltonian of this system is

$$\mathcal{H} = \sum_l \frac{p_l^2}{2m} + \sum_k \nu_{AA}^k \varepsilon_{AA}^k + \nu_{AB}^k \varepsilon_{AB}^k + \nu_{BB}^k \varepsilon_{BB}^k, \tag{1}$$

where the first sum is over all particles' momenta and the second sum is over all distances $k\eta$ to account for the interaction potential.

The total number of interactions N_{ij} between particles of type i and particles j can be written summing over all distances $k\eta$ as

$$N_{ij} = \sum_k \nu_{ij}^k. \tag{2}$$

Each pair of particles counts as one interaction: first with second, second with third, and so on. We have $N-1$ pairs, since the last particle does not interact with the first.

Thus the total number of interactions must equal $(N-1)$. Since N is considered very large, we can write $N-1 \approx N$. Hence

$$\sum_k (\nu_{AA}^k + \nu_{AB}^k + \nu_{BB}^k) = N_{AA} + N_{AB} + N_{BB} \approx N. \tag{3}$$

To find a relation between ν_{ij}^k and the system size L it is not enough to multiply the number of interactions by the site separation η, since this will not account for empty sites. We must take into account the interaction distance $k\eta$, leading to

$$\sum_k (\nu_{AA}^k + \nu_{AB}^k + \nu_{BB}^k) k\eta = L. \tag{4}$$

Finally, we want to find a relation between the number of particles and the number of cross-type interactions. An $i-i$ bond count as two i particles, while an $i-j$ $(i \neq j)$ bond count as a single particle of type i. Multiplying by 2 we can write N_A and N_B as

$$\sum_k (2\nu_{ii}^k + \nu_{ij}^k) = 2N_i. \tag{5}$$

A microscopic state of this line of particles is given by the set of values $\{\nu_{ij}^k\}$ satisfying Equations (3) to (5). Therefore, the partition function in the canonical ensemble [41] is given by

$$Z = \sum_{\{\nu_{ij}^k\}} e^{-\beta \mathcal{H}} = \frac{Q}{\Lambda^N}, \tag{6}$$

where we separated the sum into a constant originated from the kinetic energy gaussian integral given by

$$\Lambda = \left(\frac{\beta h^2}{2\pi m} \right)^{1/2} \tag{7}$$

and a configurational term defined as

$$Q = \sum_{\{\nu_{ij}^k\}^*} \Omega(\nu_{ij}^k) \exp\left(-\beta \sum_k \nu_{AA}^k \varepsilon_{AA}^k + \nu_{AB}^k \varepsilon_{AB}^k + \nu_{BB}^k \varepsilon_{BB}^k \right). \tag{8}$$

In this expression, $\Omega(\nu_{ij}^k)$ is the combinatorial factor needed to account for different configurations with the same energy. Thus, we must sum over a smaller set $\{\nu_{ij}^k\}^*$ which does not include the repeated values. To determine the factor Ω, let's begin with the simple case $N_B = 0$. This problem is analogous to distributing n balls in l boxes, where the first box contains r_1 balls, the second contains r_2 balls, and so on, with $r_1 + r_2 + \cdots + r_l = n$. Here,

we want to distribute N_{AA} between l subpopulations, given that the k-th subpopulation contains ν_{AA}^k elements. It follows that [42, p. 37]

$$\Omega = \frac{\left(\sum_k \nu_{AA}^k\right)!}{\prod_k \nu_{AA}^k!} = \frac{N_{AA}!}{\prod_k \nu_{AA}^k!} = \frac{N_A!}{\prod_k \nu_{AA}^k!}. \tag{9}$$

For two components, the AB interactions make this factor a little more complicated. Since we have N_A A-particles, we have N_A pairs of particles where the particle on the left is of type A. This results in two possible cases: the particle on the right might be A or B. Let ν_{AB}^{*k} be the number of AB interactions beginning with A at a distance $k\eta$. We want to distribute $\sum_k \nu_{AA}^k + \nu_{AB}^{*k}$ interactions, given that the k-th subpopulation contains $\nu_{AA}^k + \nu_{AB}^{*k}$ elements.

To calculate ν_{AB}^{*k}, suppose ν_{AB}^k is even and the line of particles starts with A. This means that it must also end with A. It follows that for each AB interaction (A on the left of B) there must be another BA interaction (B on the left of A). Therefore,

$$\nu_{AB}^{*k} = \frac{\nu_{AB}^k}{2}. \tag{10}$$

If ν_{AB}^k is odd we have a similar argument and find that $\nu_{AB}^{*k} = (\nu_{AB}^k + 1)/2$. Since the number of particles and interactions is large, the $1/2$ factor can be ignored.

Similarly, we count pairs starting with B and multiply these two results to obtain Ω for the mixture. Using Equation (5), this leads to

$$\Omega = \frac{N_A!}{\prod_k \nu_{AA}^k! \nu_{AB}^{*k}!} \times \frac{N_B!}{\prod_k \nu_{BB}^k! \nu_{BA}^{*k}!} = \frac{N_A! N_B!}{\prod_k \nu_{AA}^k! \nu_{BB}^k! \left[\left(\frac{\nu_{AB}^k}{2}\right)!\right]^2}. \tag{11}$$

We multiply Z by a factor $e^{-\beta PL}$ and sum over all volumes to find $Y = Y(\beta, P, N)$, the partition function in the Isothermal-Isobaric ensemble [41, p. 123]:

$$Y = \frac{1}{\Lambda^N} \sum_L e^{-\beta PL} \sum_{\{\nu_{ij}^k\}^*} \Omega(\nu_{ij}^k) \exp\left(-\beta \sum_k \nu_{AA}^k \varepsilon_{AA}^k + \nu_{AB}^k \varepsilon_{AB}^k + \nu_{BB}^k \varepsilon_{BB}^k\right).$$

To simplify the calculations, we will work with Y^*, the configurational term of this function. It is calculated by

$$Y^* = \sum_L \sum_{\{\nu_{ij}^k\}^*} \Omega(\nu_{ij}^k) \exp\left(-\beta \sum_k \nu_{AA}^k \varepsilon_{AA}^k + \nu_{AB}^k \varepsilon_{AB}^k + \nu_{BB}^k \varepsilon_{BB}^k\right) e^{-\beta PL}.$$

We use Equation (4) to replace L. This double sum is the same as summing over the set $\{\nu_{ij}^k\}^{**}$ of all configurations that satisfy Equations (3) and (5), since we lifted the constraint over L defined by Equation (4). This leads to

$$Y^* = \sum_{\{\nu_{ij}^k\}^{**}} \Omega(\nu_{ij}^k) \exp\left(-\beta \sum_k \nu_{AA}^k \varepsilon_{AA}^k + \nu_{AB}^k \varepsilon_{AB}^k + \nu_{BB}^k \varepsilon_{BB}^k\right) \times \\ \times \exp\left(-\beta P \sum_k (\nu_{AA}^k + \nu_{AB}^k + \nu_{BB}^k) k\eta\right).$$

As typical in Statistical Mechanics, we approximate this sum by its largest term representing the equilibrium configuration. Hence,

$$Y^* \approx \Omega(\nu_{ij}^k) e^{\left(-\beta \sum_k \nu_{AA}^k \varepsilon_{AA}^k + \nu_{AB}^k \varepsilon_{AB}^k + \nu_{BB}^k \varepsilon_{BB}^k - (\nu_{AA}^k + \nu_{AB}^k + \nu_{BB}^k) Pk\eta\right)}.$$

To find the equilibrium values of ν_{ij}^k, $\ln(Y^*)$ must be extremized. To satisfy the constraints defined by Equation (5), we introduce the Lagrange Multipliers λ_1 and λ_1. Thus we must solve

$$\begin{aligned} \delta[\ln Y^* + \\ &+ \lambda_1 \sum_k (2\nu_{AA}^k + \nu_{AB}^k) \\ &+ \lambda_2 \sum_k (2\nu_{BB}^k + \nu_{AB}^k) \\ ] = 0. \end{aligned} \tag{12}$$

Writing the terms explicitly, using the Stirling approximation, removing the constants and grouping in terms of each ν_{ij}^k leads to

$$\begin{aligned} \delta[\\ &\sum_k \nu_{AA}^k [-\beta(\varepsilon_{AA}^k + Pk\eta) + 2\lambda_1 - \ln(\nu_{AA}^k)] + \\ &\sum_k \nu_{BB}^k [-\beta(\varepsilon_{BB}^k + Pk\eta) + 2\lambda_2 - \ln(\nu_{BB}^k)] + \\ &\sum_k \nu_{AB}^k [-\beta(\varepsilon_{AB}^k + Pk\eta) + \lambda_1 + \lambda_2 - \ln(\nu_{AB}^k)] \\ ] = 0. \end{aligned} \tag{13}$$

To satisfy this equation, it is sufficient that

$$\nu_{AA}^k = \exp\left[-\beta(\varepsilon_{AA}^k + Pk\eta) + 2\lambda_1\right], \tag{14}$$

$$\nu_{BB}^k = \exp\left[-\beta(\varepsilon_{BB}^k + Pk\eta) + 2\lambda_2\right], \tag{15}$$

$$\nu_{AB}^k = \exp\left[-\beta(\varepsilon_{AB}^k + Pk\eta) + \lambda_1 + \lambda_2\right]. \tag{16}$$

Now we replace these equilibrium values of ν_{ij}^k inside the $\ln(\nu_{ij}^k)$ terms in $\ln Y^*$. The terms $(\varepsilon_{ij}^k + Pk\eta)$ will cancel out. Therefore,

$$\ln Y^* = N + \ln(N_A!) + \ln(N_B!) - 2\lambda_1 N_{AA} - 2\lambda_2 N_{BB} - (\lambda_1 + \lambda_2) N_{AB}. \tag{17}$$

Note that

$$N_{AA} = \sum_k \nu_{AA}^k = \sum_k e^{-\beta\varepsilon_{AA}^k - \beta Pk\eta + 2\lambda_1} = e^{2\lambda_1}\varphi_{AA}, \tag{18}$$

where we define

$$\varphi_{ij} \equiv \sum_k e^{-\beta(\varepsilon_{ij}^k + Pk\eta)}. \tag{19}$$

Using the analogous relations for N_{AB} and N_{BB} we conclude that

$$2\lambda_1 = \ln\left(\frac{N_{AA}}{\varphi_{AA}}\right), \tag{20}$$

$$2\lambda_2 = \ln\left(\frac{N_{BB}}{\varphi_{BB}}\right), \tag{21}$$

$$\lambda_1 + \lambda_2 = \ln\left(\frac{N_{AB}}{\varphi_{AB}}\right), \tag{22}$$

which implies

$$\begin{aligned}\ln Y^* =& N + \ln(N_A!) + \ln(N_B!) \\ &- N_{AA}\ln\left(\frac{N_{AA}}{\varphi_{AA}}\right) - N_{BB}\ln\left(\frac{N_{BB}}{\varphi_{BB}}\right) - N_{AB}\ln\left(\frac{N_{AB}}{\varphi_{AB}}\right).\end{aligned}$$

Since $N = N_{AA} + N_{AB} + N_{BB}$, we use the Stirling approximation in reverse to recover the factorials of N_{AA}, N_{AB} and N_{BB}. Including the Λ term and exponentiating both sides of the equation leads to [39, 40]:

$$Y(\beta, P, N) = \frac{1}{\Lambda^N} \frac{N_A! N_B!}{N_{AA}! N_{BB}! \left[\left(\frac{N_{AB}}{2}\right)!\right]^2} \times \varphi_{AA}^{N_{AA}} \varphi_{AB}^{N_{AB}} \varphi_{BB}^{N_{BB}}. \tag{23}$$

We can also use this formalism to describe continuous systems in the limit of $\eta \to 0$ when the sites become arbitrarily close. This suggests the substitutions

$$k\eta \to r, \tag{24}$$

$$\varepsilon_{ij}^{k} \to \varepsilon_{ij}(r), \tag{25}$$

$$\nu_{ij}^{k} \to \nu_{ij}(r). \tag{26}$$

Thus we must replace the sum in φ_{ij} by an integral defined by

$$\varphi_{ij} = \int_0^\infty e^{-\beta(\varepsilon_{ij}(r)+Pr)} dr. \tag{27}$$

The connection between the Isothermal-Isobaric Ensemble and Thermodynamics is made through the Gibbs Free Energy [41, p. 124]

$$g(\beta, P) = -\frac{1}{\beta} \lim_{N\to\infty} \left[\frac{\ln Y(\beta, P, N)}{N} \right]. \tag{28}$$

This allows us, in turn, to find the thermodynamical quantities of interest, such as [43, p. 84, p. 170]

$$\begin{aligned} v &= \left(\frac{\partial g}{\partial P} \right)_\beta, \\ s &= -\left(\frac{\partial g}{\partial T} \right)_P, \\ c_p &= \frac{1}{T} \left(\frac{\partial s}{\partial T} \right)_P, \\ h &= g + Ts, \end{aligned}$$

where $T = (k_B\beta)^{-1}$.

We can also find the excess thermodynamic quantities. The excess of some value z is a function of the concentration of each species. It is defined as z minus the value that z would assume in an ideal mixture:

$$z^E(x_A, x_B) = z(x_A, x_B) - [x_A z(x_A = 1, x_B = 0) + x_B z(x_A = 0, x_B = 1)].$$

Note that we can write g more explicitly as

$$\begin{aligned} g &= \frac{1}{\beta} \ln \Lambda - \frac{1}{\beta} \lim_{N\to\infty} \frac{1}{N} \ln Y^* \\ &= \frac{1}{\beta} \ln \Lambda - \frac{1}{\beta} \lim_{N\to\infty} \left[\frac{\Delta}{N} + \frac{N_{AA} \ln \varphi_{AA} + N_{AB} \ln \varphi_{AB} + N_{BB} \ln \varphi_{BB}}{N} \right], \end{aligned} \tag{29}$$

where

$$\Delta \equiv \ln\left[\frac{N_A!N_B!}{N_{AA}!N_{BB}!\left[\left(\frac{N_{AB}}{2}\right)!\right]^2}\right]$$
$$= N_A \ln N_A + N_B \ln N_B - N_{AA} \ln N_{AA} - N_{BB} \ln N_{BB} - N_{AB} \ln\left(\frac{N_{AB}}{2}\right).$$

In this expression, we can find φ_{ij} integrating the potential. We also known the concentrations of each species, $x_A = N_A/N$ and $x_B = N_B/N$. But it is not obvious what is the limiting behavior of the terms $\frac{N_{ij}}{N}$. Let

$$x_{ij} = \lim_{N\to\infty} \frac{N_{ij}}{N} \tag{30}$$

be the ij interaction ratio. Our first attempted solution is to approximate these ratios.

2.2 Random Mixing approximation

In our system, x_{ij} represents the fraction of interactions of type ij in relation to the total number of interactions. If we have N_A and N_B particles distributed randomly in a line, this is equivalent to the probability of having a particle of type i at the side of a particle of type j. Therefore,

$$x_{AA} = \frac{N_A}{N} \times \frac{N_A}{N}, \tag{31}$$
$$x_{BB} = \frac{N_B}{N} \times \frac{N_B}{N}, \tag{32}$$
$$x_{AB} = 2\frac{N_A}{N} \times \frac{N_B}{N}, \tag{33}$$

where we used a factor of 2 in the last equation to account for AB and BA interactions. This leads to

$$\Delta = -N_A \ln x_A - N_B \ln x_B. \tag{34}$$

Replacing this result in g and also using the random mixing approximation for constants multiplying the $\ln(\varphi_{ij})$ terms, we find that

$$g = \frac{1}{\beta}\ln\Lambda - \frac{1}{\beta}(-x_A \ln x_A - x_B \ln x_B + x_A^2 \ln\varphi_{AA} + 2x_A x_B \ln\varphi_{AB} + x_B^2 \ln\varphi_{BB}).$$

We define $x \equiv x_B = 1 - x_A$. Since the first three terms don't depend on P the volume is expressed as

$$v = -\frac{1}{\beta}\left[\frac{(1-x)^2}{\varphi_{AA}}\left(\frac{\partial\varphi_{AA}}{\partial P}\right)_\beta + \frac{2x(1-x)}{\varphi_{AB}}\left(\frac{\partial\varphi_{AB}}{\partial P}\right)_\beta + \frac{x^2}{\varphi_{BB}}\left(\frac{\partial\varphi_{BB}}{\partial P}\right)_\beta\right]. \tag{35}$$

From Equation (35) the excess volume becomes a very simple expression:

$$\begin{aligned} v^E =& v - [(1-x)v_A + xv_B] \\ =& -\frac{(1-x)^2}{\beta\varphi_{AA}}\left(\frac{\partial\varphi_{AA}}{\partial P}\right)_\beta - \frac{2(1-x)x}{\beta\varphi_{AB}}\left(\frac{\partial\varphi_{AB}}{\partial P}\right)_\beta - \frac{x^2}{\beta\varphi_{BB}}\left(\frac{\partial\varphi_{BB}}{\partial P}\right)_\beta \\ &+ \frac{(1-x)}{\beta\varphi_{AA}}\left(\frac{\partial\varphi_{AA}}{\partial P}\right)_\beta + \frac{x}{\beta\varphi_{BB}}\left(\frac{\partial\varphi_{BB}}{\partial P}\right)_\beta \\ =& (\phi_{AA} + \phi_{BB} - 2\phi_{AB})(x^2 - x), \end{aligned} \tag{36}$$

where

$$\phi_{ij} = -\frac{1}{\beta\varphi_{ij}}\left(\frac{\partial\varphi_{ij}}{\partial P}\right)_\beta. \tag{37}$$

After finding the entropy, the calculation process for h^E is analogous to v^E. Again, we group in powers of x to find a quadratic equation:

$$\begin{aligned} h^E &= h - [(1-x)h_A + xh_B] \\ &= (\phi'_{AA} + \phi'_{BB} - 2\phi'_{AB})(x^2 - x), \end{aligned} \tag{38}$$

where

$$\phi'_{ij} = -\frac{1}{\varphi_{ij}}\left(\frac{\partial\varphi_{ij}}{\partial\beta}\right)_P. \tag{39}$$

The same quadratic pattern happens in the excess specific heat. It follows that the maximum or minimum of these excess quantities always happens at $x = 0.5$ for any potential. The concavity can be controlled from the potential parameters, which modify the signal of the x^2 coefficients, but this approximation does not capture the change in the concentration at which the maximum happens for different temperatures.

To find the temperature of maximum density, we use the φ_{ij} to calculate the volume and minimize $v = v(\beta, P)$ for a given pressure. To simplify our results, we adopt a unit system such that $k_B = h = 1$. Define the potential $\varepsilon(r)$ as:

$$\varepsilon(r,i,j) = \begin{cases} \varepsilon_{AA}(r), & \text{if } i = j = A \\ \varepsilon_{BB}(r), & \text{if } i = j = B \\ \varepsilon_{AB}(r), & \text{if } i \neq j \end{cases}, \tag{40}$$

where

$$\varepsilon_{ij}(r) = \begin{cases} 0, & \text{if } r > c_{ij} \\ a_{ij}, & \text{if } b_{ij} < r < c_{ij} \\ \infty, & \text{if } r < b_{ij} \end{cases} . \tag{41}$$

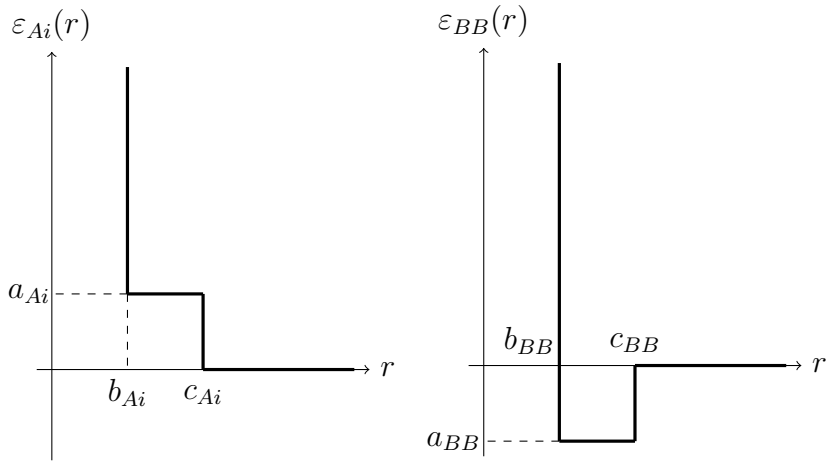

Figure 5: Potential for AA, AB (left) and BB (right) interactions

For this simple potential, we have 9 parameters: a, b and c for each type of interaction AA, AB and BB. Calculating φ_{ij} for this potential we find that

$$\varphi_{ij} = \frac{e^{-\beta a_{ij}}(e^{-\beta P b_{ij}} - e^{-\beta P c_{ij}}) + e^{-\beta P c_{ij}}}{\beta P}. \tag{42}$$

We know that the set of parameters $a_{AA} = 1, b_{AA} = 1, c_{AA} = 1.8$ displays a water-like density anomaly for a pure fluid [37]. We fix these parameter and iterate over ranges of a_{ij}, b_{ij} and c_{ij} for the AB and BB interactions. For each set of parameters, we search for a local minimum of v, as shown in Figure 6. Iterating over the desired concentrations, we are able to plot ΔTMD, as shown in Figure 7. This was done in Python with Sympy and SciPy libraries [44, 45]. The parameters used in the figures were $a_{AB} = 1, a_{BB} = -2, b_{AB} = 1.2, b_{BB} = 2.5, c_{AB} = 2$ and $c_{BB} = 2.9$.

Table 1 shows details about the tested range of parameters, which were calculated for two different pressures. In total, 3231900 sets were tested. We were unable to find parameters that result in a positive TMD. Therefore, this random mixing approximation appears insufficient to capture the increase of the TMD in the high dilution regime which

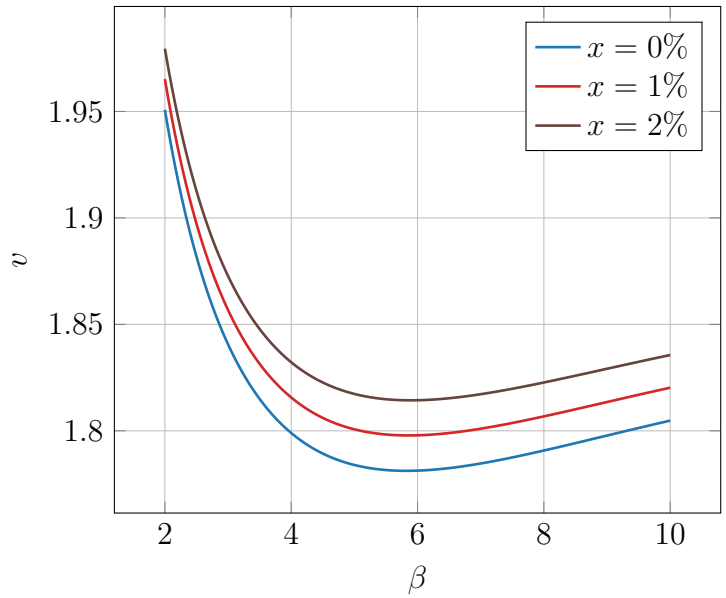

Figure 6: Volume for different concentrations in the random mixing solution ($P = 1$).

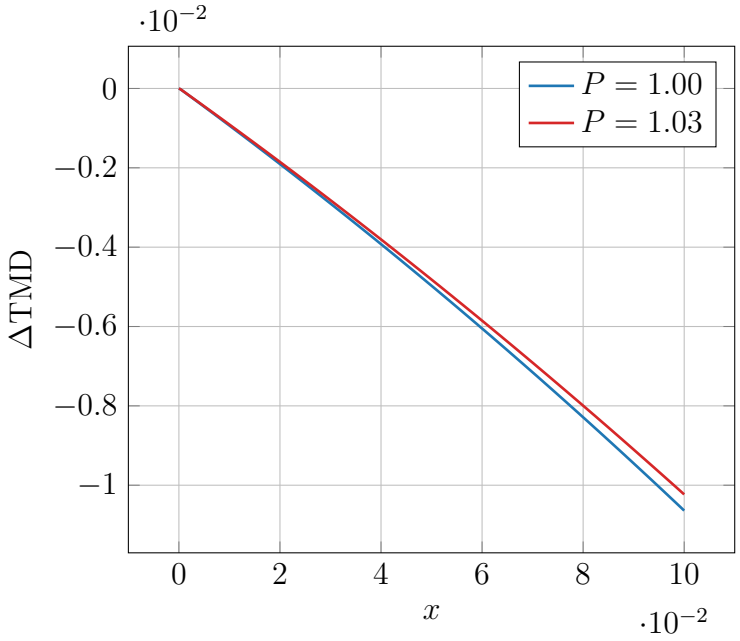

Figure 7: ΔTMD in the random mixing solution.

Parameter	Initial value	Final value	Increment
a_{BB}	-2	-0.1	0.1
b_{BB}	$b_{AA} + 0.1$	3	0.1
c_{BB}	$b_{BB} + 0.1$	$b_{BB} + 1$	0.1
a_{AB}	0.1	$a_{AA} - 0.1$	0.1
b_{AB}	$b_{AA} + 0.1$	b_{BB}	0.1
c_{AB}	$b_{AB} + 0.1$	$b_{AB} + 1$	0.1
x	0	0.1	0.01

Table 1: Range of values used in the ΔTMD calculation.

characterizes the "structure-maker" alcohols. We have also seen that it does not reproduce the interesting behaviors of the excess quantities. This suggests the necessity of finding the exact values of the interaction ratios x_{ij}.

2.3 The exact interation ratios

In the continuous limit, we can write Equation (2) as

$$N_{ij} = \int_0^\infty \nu_{ij}(r)dr. \tag{43}$$

We can also rewrite Equations (14) to (16) as

$$\nu_{AA}(r) = e^{-\beta[\varepsilon_{AA}(r)+Pr]}e^{2\lambda_1}, \tag{44}$$

$$\nu_{BB}(r) = e^{-\beta[\varepsilon_{BB}(r)+Pr]}e^{2\lambda_2}, \tag{45}$$

$$\nu_{AB}(r) = e^{-\beta[\varepsilon_{AB}(r)+Pr]}e^{\lambda_1+\lambda_2}. \tag{46}$$

Replacing Equations (44) to (46) in Equation (5) results in a coupled system of quadratic equations defined by

$$\begin{cases} \varphi_{AA}e^{2\lambda_1} + \varphi_{AB}e^{\lambda_2}e^{\lambda_1} - N_A = 0 \\ \varphi_{BB}e^{2\lambda_2} + \varphi_{AB}e^{\lambda_1}e^{\lambda_2} - N_B = 0 \end{cases}. \tag{47}$$

The Lagrange multipliers λ_1 and λ_2 are found from this system of equations. The

result is

$$e^{2\lambda_1} = \frac{(N_A - N_B) - 2N_A\gamma + \sqrt{(N_A - N_B)^2 + 4N_A N_B \gamma}}{2\varphi_{AA}\,(1-\gamma)}, \tag{48}$$

$$e^{2\lambda_2} = \frac{-(N_A - N_B) - 2N_B\gamma + \sqrt{(N_A - N_B)^2 + 4N_A N_B \gamma}}{2\varphi_{BB}\,(1-\gamma)}, \tag{49}$$

where we defined

$$\gamma \equiv \frac{\varphi_{AA}\varphi_{BB}}{\varphi_{AB}^2}. \tag{50}$$

From Equations (20) and (21),

$$N_{AA} = e^{2\lambda_1}\varphi_{AA}, \tag{51}$$

$$N_{BB} = e^{2\lambda_2}\varphi_{BB}. \tag{52}$$

We can divide each of these equations by N and find the exact solution for this system. The result is

$$x_{AA} = \lim_{N\to\infty}\frac{N_{AA}}{N} = \frac{(x_A - x_B) - 2x_A\gamma + \sqrt{(x_A - x_B)^2 + 4x_A x_B \gamma}}{2\,(1-\gamma)}, \tag{53}$$

$$x_{BB} = \lim_{N\to\infty}\frac{N_{BB}}{N} = \frac{-(x_A - x_B) - 2x_B\gamma + \sqrt{(x_A - x_B)^2 + 4x_A x_B \gamma}}{2\,(1-\gamma)}, \tag{54}$$

$$x_{AB} = \lim_{N\to\infty}\frac{N_{AB}}{N} = 2(x_A - x_{AA}), \tag{55}$$

where we used $N_{AB} = 2(N_A - N_{AA})$ from Equation (5).

This means that the limiting behavior of x_{ij} is a quantity that depends only on the potential integrals $\varphi_{ij} = \varphi_{ij}(\beta, P)$ and the concentration x. Manipulating Equation (29) and using $x \equiv x_B = 1 - x_A$ we find the exact Gibbs Free Energy for this system:

$$\begin{aligned} g =& \frac{1}{\beta}\ln\Lambda - \frac{1}{\beta}[(1-x)\ln(1-x) + x\ln(x) - x_{AA}\ln(x_{AA}) - x_{BB}\ln(x_{BB}) \\ & - x_{AB}\ln(x_{AB}/2) + x_{AA}\ln(\varphi_{AA}) + x_{BB}\ln(\varphi_{BB}) + x_{AB}\ln(\varphi_{AB})]. \end{aligned} \tag{56}$$

We repeated the process done for the previous approximation. Minimizing $v = v(\beta, p)$ to find a local minimum as shown in Figure 9, we get the temperature of maximum density for each solute concentration x. In this exact solution, we were able to find sets of parameters that reproduce the increase in the TMD, even for this simple model. We restricted our search to the sets such that the curve for the higher pressure is below the

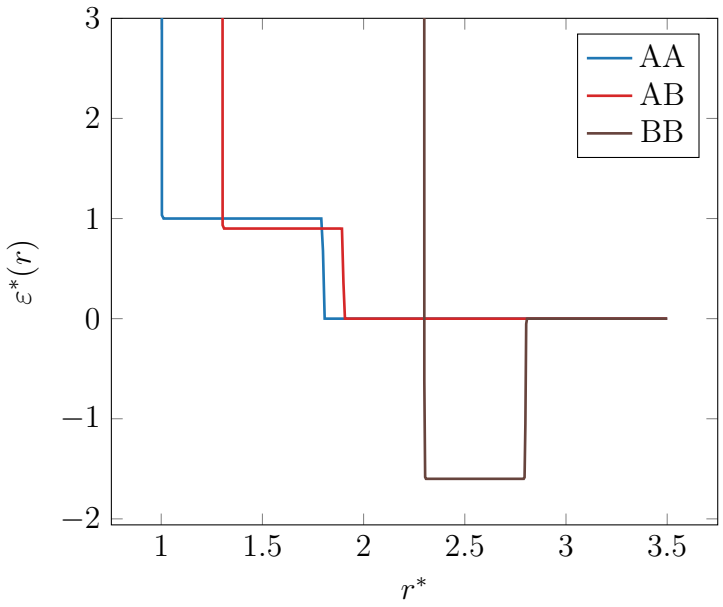

Figure 8: Discontinuous CS potential in reduced units.

curve for the lower pressure. This behavior is confirmed in simulations [46]: a higher pressure tends to destroy the low-density structures of water, hence a smaller temperature is necessary to reach the maximum density. One of these sets is plotted in Figure 10. We used $a_{AB} = 0.9, a_{BB} = -1.6, b_{AB} = 1.3, b_{BB} = 2.3, c_{AB} = 1.9, c_{BB} = 2.8$. The potential generated by these parameters is shown in Figure 8.

The behavior for this exact solution is what we would expect based on the experiments: a region of positive ΔTMD for small solute concentrations. The tested range of parameters was the same as defined for the random mixing case (see Table 1). In total, 10765 sets of parameters were found which increased the TMD.

In the exact solution, we could not find a simple expression for the volume and the excess quantities as we did in the approximated case. Hence, the excess quantities must be studied numerically. Differently from experimental results, the model presents symmetric curves as a function of concentration: all tested parameters display a maximum or minimum at $x = 0.5$. Figure 11 displays v^E, h^E and c_P^E for the same parameter set of Figure 10.

We were not able to find parameters that change the concavity of the excess enthalpy while retaining the increase in the TMD for low concentrations. On the other hand, it is possible to make the excess volume positive, as shown in Figure 12 for $a_{AB} = 0.4, a_{BB} = -1.2, b_{AB} = 1.9, b_{BB} = 2.7, c_{AB} = 2.8, c_{BB} = 3.1$. For this set of parameters we also have

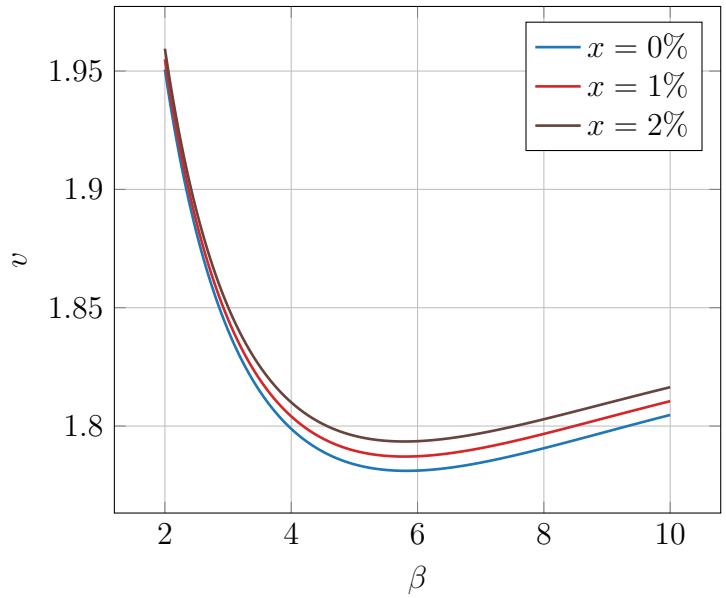

Figure 9: Volume for different concentrations in the exact solution ($P = 1$).

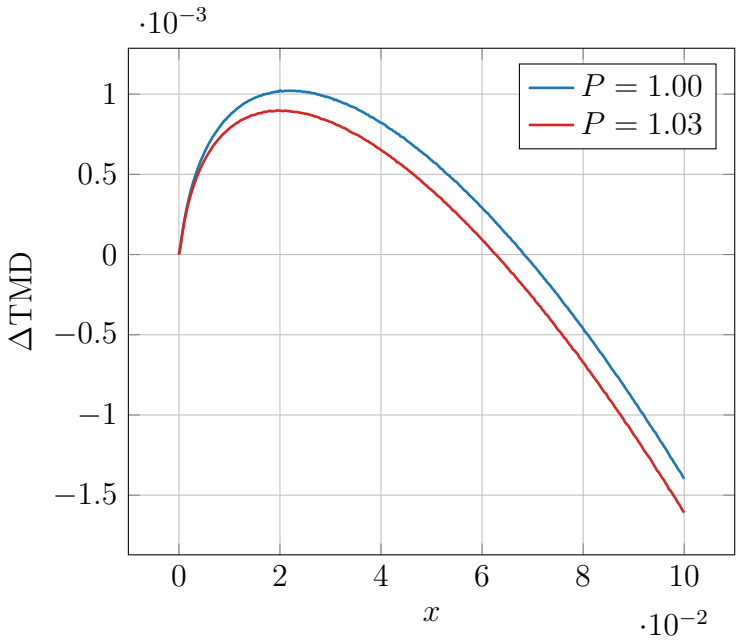

Figure 10: ΔTMD in the exact solution.

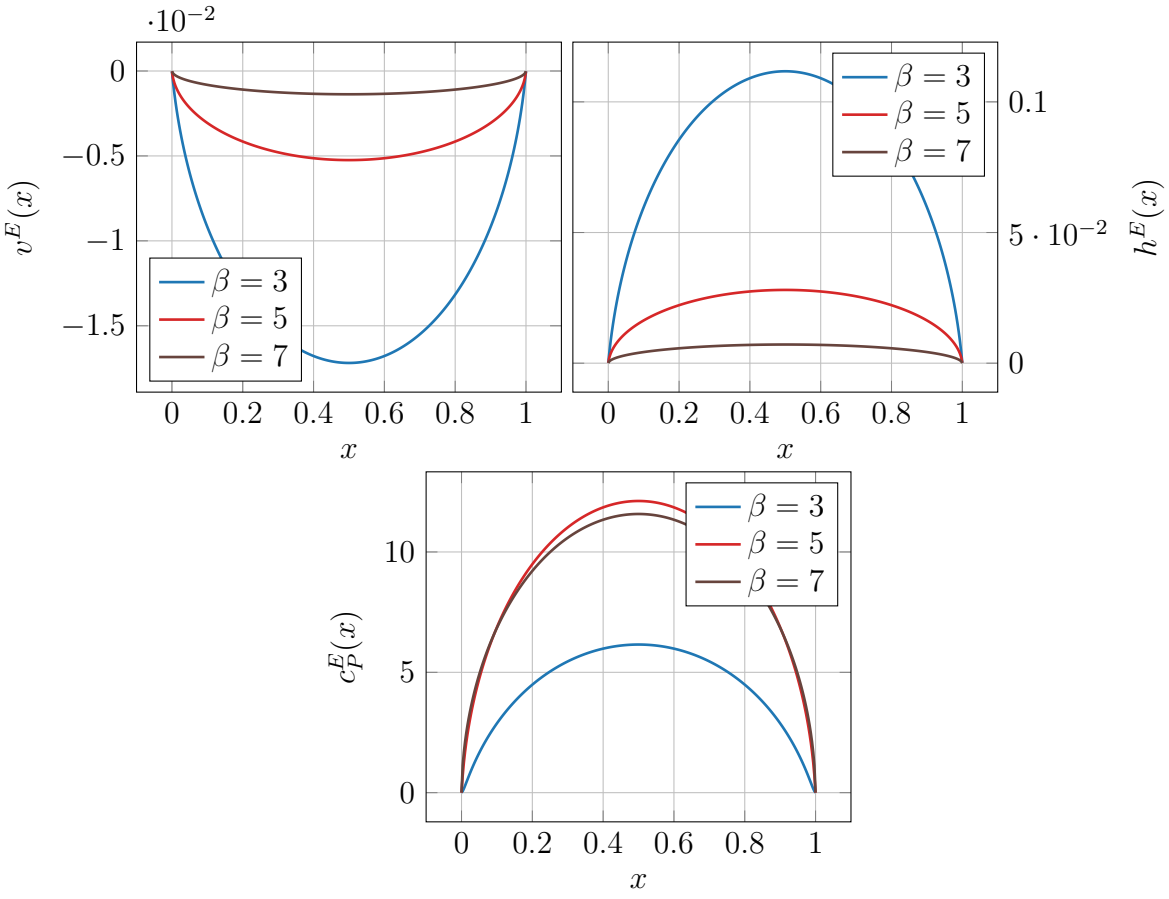

Figure 11: Excess quantities in the exact solution.

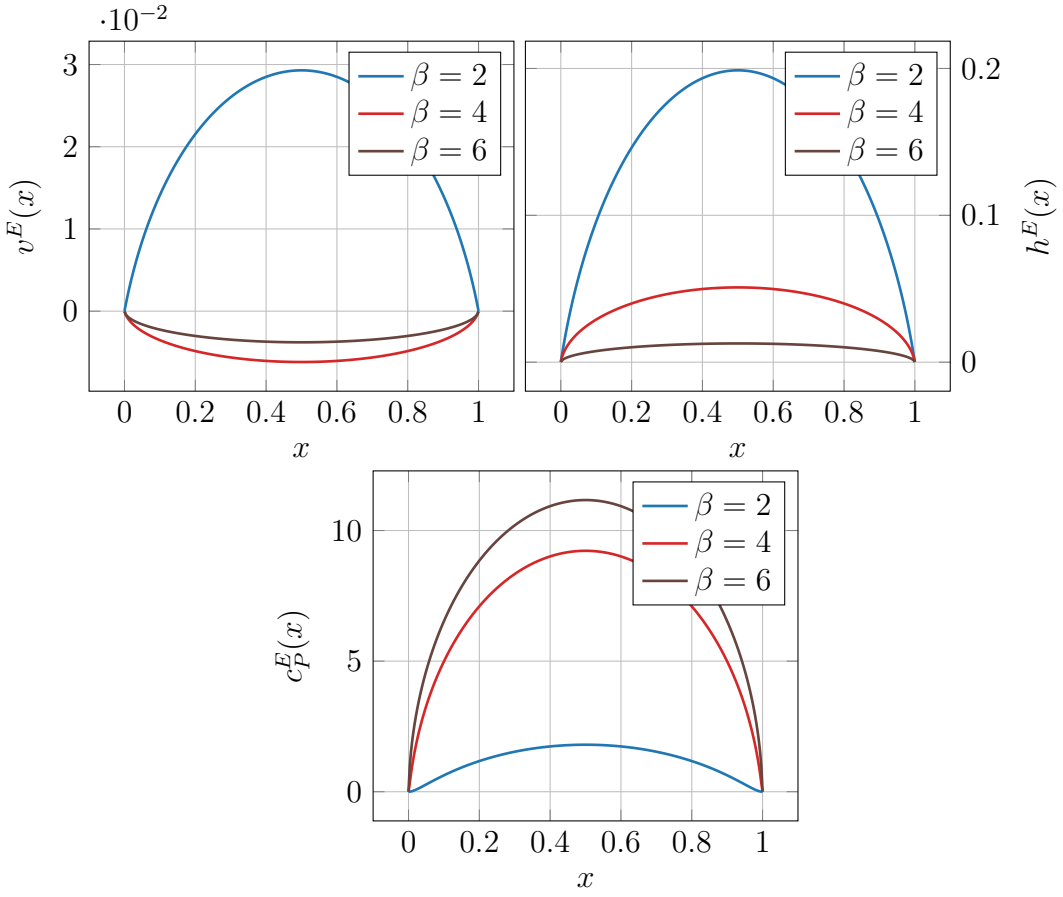

Figure 12: Excess quantities in the exact solution with positive excess volume.

an increase in ΔTMD similar to Figure 10.

Thus, we were able to show that, even for this one-dimensional model using a simple CS potential, it is possible to have an increase in the temperature of maximum density with the increase of solute concentration. On the other hand, this system appears unable to reproduce the asymmetry found in the excess quantities, with maximum or minimum values at concentrations different than 0.5.

3 Molecular Dynamics Simulations

The next step is to understand if the $\Delta\text{TMD} > 0$ behavior is a general property of this type of potential or if this result is only present in the one-dimensional model. Since we do not have an exact solution in three dimensions, we use simulations to study this system.

3.1 General Method

Molecular Dynamics (MD) is a widely used simulation technique [47] to investigate thermodynamic properties of a system such as water anomalies. It is based on the ergodicity principle, allowing the calculation of the ensemble average behavior of particles through the time average of the system.

More precisely, let f be some quantity of interest. To determine f in the lab we measure the time average of f over a period T which is very large in comparison with the microscopic time scale. This is expressed by

$$\langle f \rangle_T = \lim_{T\to\infty} \frac{1}{T} \int_0^T f(t)dt. \tag{57}$$

On the other hand, the average over the phase space Ω is given by

$$\langle f \rangle_\Omega = \int_\Omega f(\omega)d\omega. \tag{58}$$

If the probability of the system visiting each configuration is the same, it is reasonable to assume that

$$\langle f \rangle_T = \langle f \rangle_\Omega, \tag{59}$$

which is called the ergodicity principle [41]. This means that to discover the thermodynamic properties of a system, we just need to follow its evolution over time and calculate the average of the desired quantity.

Besides quantities such as pressure, temperature and volume, MD can also be used to understand the local structure of a simulated fluid through the radial distribution function (RDF) $g(r)$ [47, p. 85]. The idea is to fix a particle and to create a histogram of the number of neighbors for each distance bin. This is represented in Figure 13[2]. Doing this process for all atoms gives us an average density as a function of distance from a particle,

[2]Adapted from https://commons.wikimedia.org/wiki/File:Rdf_schematic.svg

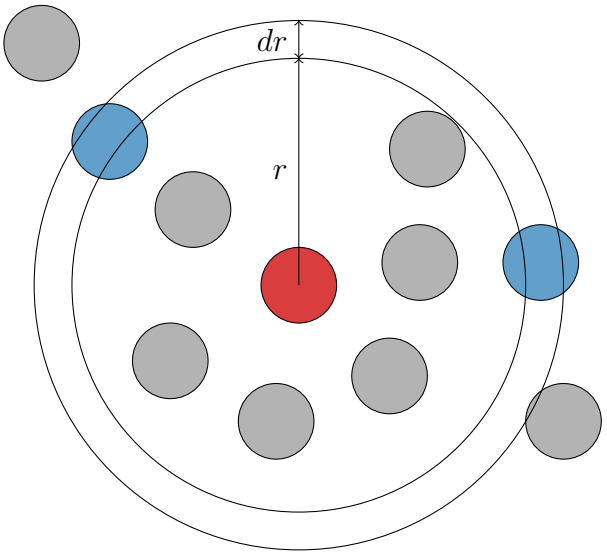

Figure 13: Two dimensional binning: counting neighbors of the red particle to calculate the Radial Distribution Function. The center of blue particles is between r and $r + dr$.

which is normalized by the ideal gas density. This is useful, for instance, to understand how the solute is organized in relation to the solvent particles.

3.2 Reduced unit system

In the following analysis, we adopt ϵ and σ as the fundamental units of energy and distance. This allows us to express all quantities in reduced units [47, p. 40], given by

$$r^* = \frac{r}{\sigma}, \qquad \varepsilon^* = \frac{\varepsilon}{\epsilon}, \qquad T^* = \frac{k_B T}{\epsilon}, \qquad \rho^* = \rho\sigma^3, \qquad P^* = \frac{P\sigma^3}{\epsilon}. \tag{60}$$

We assume all particles have unitary mass. The values of ϵ and σ are chosen from quantities that characterize the interaction potential. For instance, in the potential defined by Equation (41), a and b are convenient values of ϵ and σ, respectively. These new units are useful for molecular dynamics simulations because, in reduced units, most quantities are expressed as numbers between 10^{-3} and 10^3. This avoids rounding errors from working with very large or very small numbers in SI units.

3.3 Simulation description

The potential defined in Equation (41) does not have a density anomaly in three dimensions [48]. We define a similar potential inspired by [49] to describe the solvent-

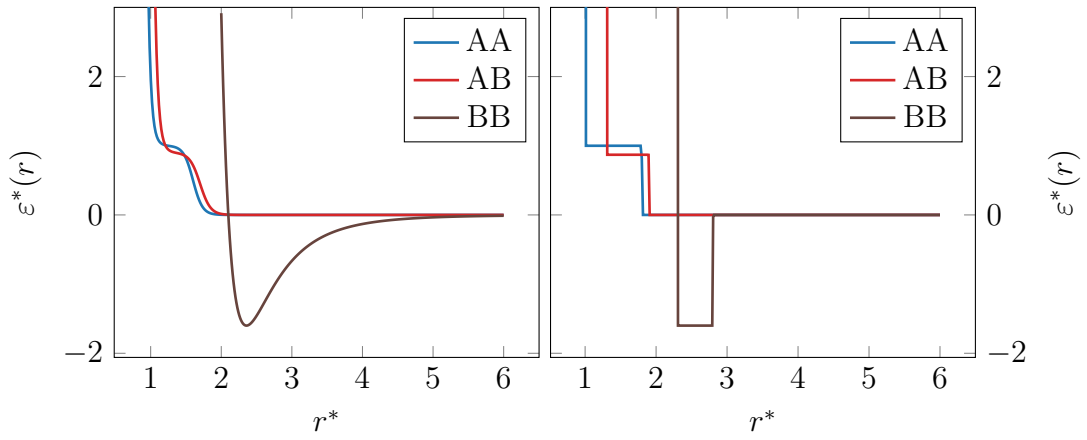

Figure 14: Continuous core-softened potential in reduced units (left) and discontinuous version from Figure 8 (right).

solvent and solvent-solute interactions, given by

$$\varepsilon_{\mathrm{Ai}}(r) = \frac{\epsilon_{\mathrm{Ai}}}{1 + \exp\left[\Delta(r - R_{\mathrm{Ai}})\right]} + \left(\frac{\sigma_{\mathrm{Ai}}}{r}\right)^{24}. \tag{61}$$

The BB interaction is described with the standard 12-6 Lennard-Jonnes potential:

$$\varepsilon_{BB}(r) = 4\epsilon_{\mathrm{BB}}\left[\left(\frac{\sigma_{\mathrm{BB}}}{r}\right)^{12} - \left(\frac{\sigma_{\mathrm{BB}}}{r}\right)^{6}\right] \tag{62}$$

We define $\Delta = 15$ to ensure a smooth potential. We also set $\sigma = \sigma_{\mathrm{AA}}$ and $\epsilon = \epsilon_{\mathrm{AA}}$ as the basic units of distance and energy. Guided by the parameters found in the one dimensional analysis, we choose $R_{\mathrm{AA}} = 1.6$, $R_{\mathrm{AB}} = 1.7$, $\sigma_{\mathrm{AB}} = 1.1$, $\sigma_{\mathrm{BB}} = 2.3$, $\epsilon_{\mathrm{AB}} = 0.9$ and $\epsilon_{\mathrm{BB}} = -1.6$. The resulting potential is compared with the 1D case in Figure 14.

We performed the molecular dynamics simulations using the LAMMPS [50] package in the NPT ensemble with the Nose-Hoover thermostat and barostat. The execution for multiple input parameters was managed with GNU Parallel [51]. The system consisted of $N = 1000$ particles in a cubic box with periodic boundary conditions. Starting from a cubic periodic lattice, we melted it with a high temperature ($T^* = 10$) using a $\delta t^* = 0.001$ timestep. Then we gradually reduced T^* until the desired simulation temperature was reached. From this state, we ran 10^6 equilibration steps followed by 2×10^6 steps for taking averages with a $\delta t^* = 0.002$ timestep. The potentials were defined through a table pair style with linear interpolation between points. We also selected three pressures in the TMD region and ran simulations adding solute from $x = 1\%$ to $x = 5\%$ with 1%

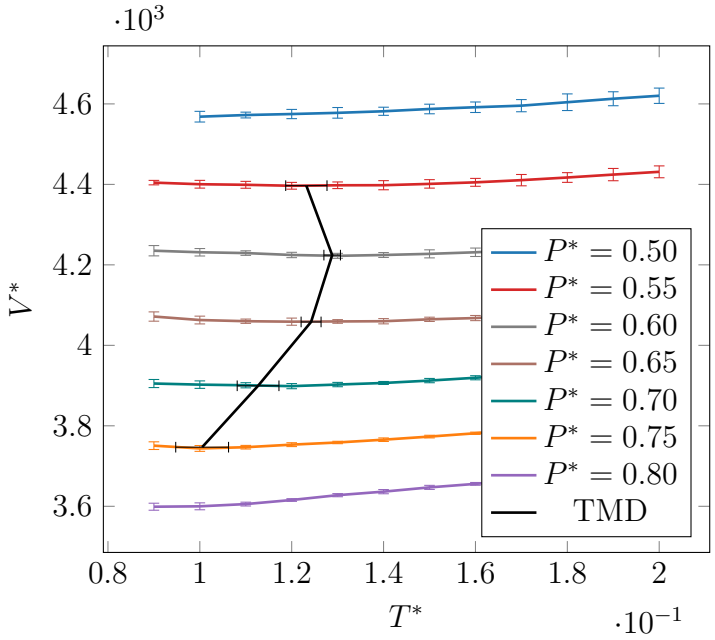

Figure 15: $V^* \times T^*$ diagram for the pure A system.

increments. In this mixture, xN particles were randomly selected from the initial periodic lattice and defined as solute.

3.4 Results

We begin with the $V^* \times T^*$ diagram shown in Figure 15. For this potential, the TMD line is located close to the region defined by $0.55 \leq P^* \leq 0.75$ and $0.10 \leq T^* \leq 0.13$. We fitted each curve using a third-degree polynomial to determine the temperature of maximum density.

The error bars in the TMD were estimated by fitting $V + \Delta V$ and $V - \Delta V$, where ΔV is the standard deviation of the volume. This gives us an upper and lower limit on the temperature of maximum density. ΔV was calculated from the fluctuation of volume of the time averages of the simulation, as shown by the error bars of Figure 15.

Figure 16 displays the radial distribution function for solvent-solvent and solvent-solute pairs. We can identify the structuring related to the two distance scales close to $r^* = 1$ and $r^* = 2$, with a non-null minimum between those maxima.

Figure 17 displays selected simulation snapshots for the system in the TMD region of the $V^* \times T^*$ diagram. Considering the periodic boundary conditions, we see that for

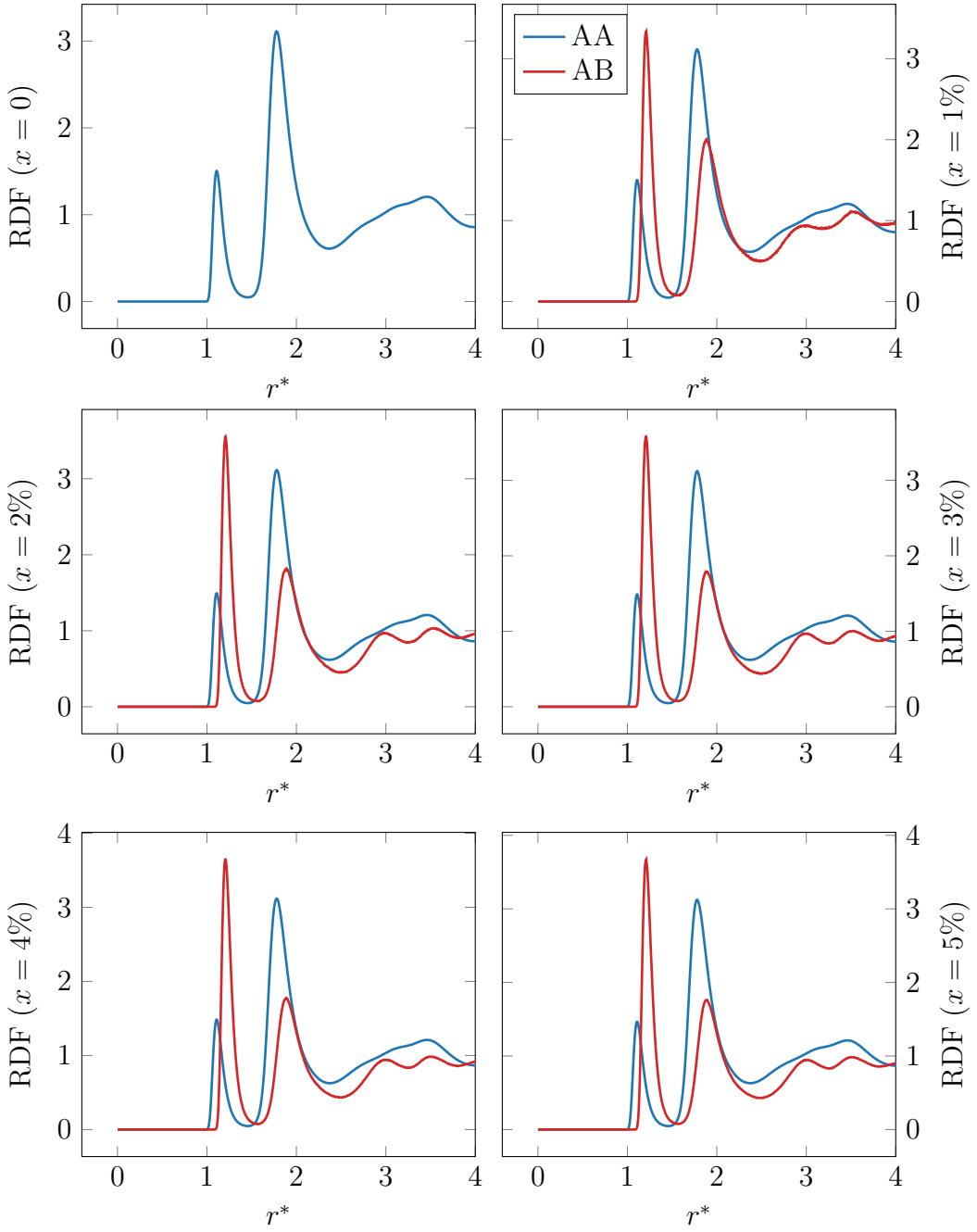

Figure 16: AA and AB Radial Distribution Function in the TMD region ($P^* = 0.70$ and $T^* = 0.11$) for different concentrations.

all concentrations the solute form clusters. This can also be seen from the BB Radial Distribution function in Figure 18, which displays high peaks in comparison with Figure 16.

The same fitting process used in the pure solvent $V^* \times T^*$ was applied for the mixture. This allows us to plot ΔTMD by subtracting the temperature of maximum density of $x = 0$. The result is shown in Figure 19. For this choice of parameters the simulation was not able to reproduce the results found in the one-dimensional case: ΔTMD goes down for all calculated pressures. Thus, with this potential, the solute act as a structure breaker.

We also analyzed the excess volume and enthalpy for the mixture simulation. Figure 20 shows V^{*E} and H^{*E} for $P^* = 0.65$. We verified that the behavior is qualitatively the same for $P^* = 0.70$ and $P^* = 0.75$: the excess volume is negative for all simulated temperatures, with a minimum around $x = 40\%$, while the excess enthalpy shifts from positive to negative with increasing solute concentration.

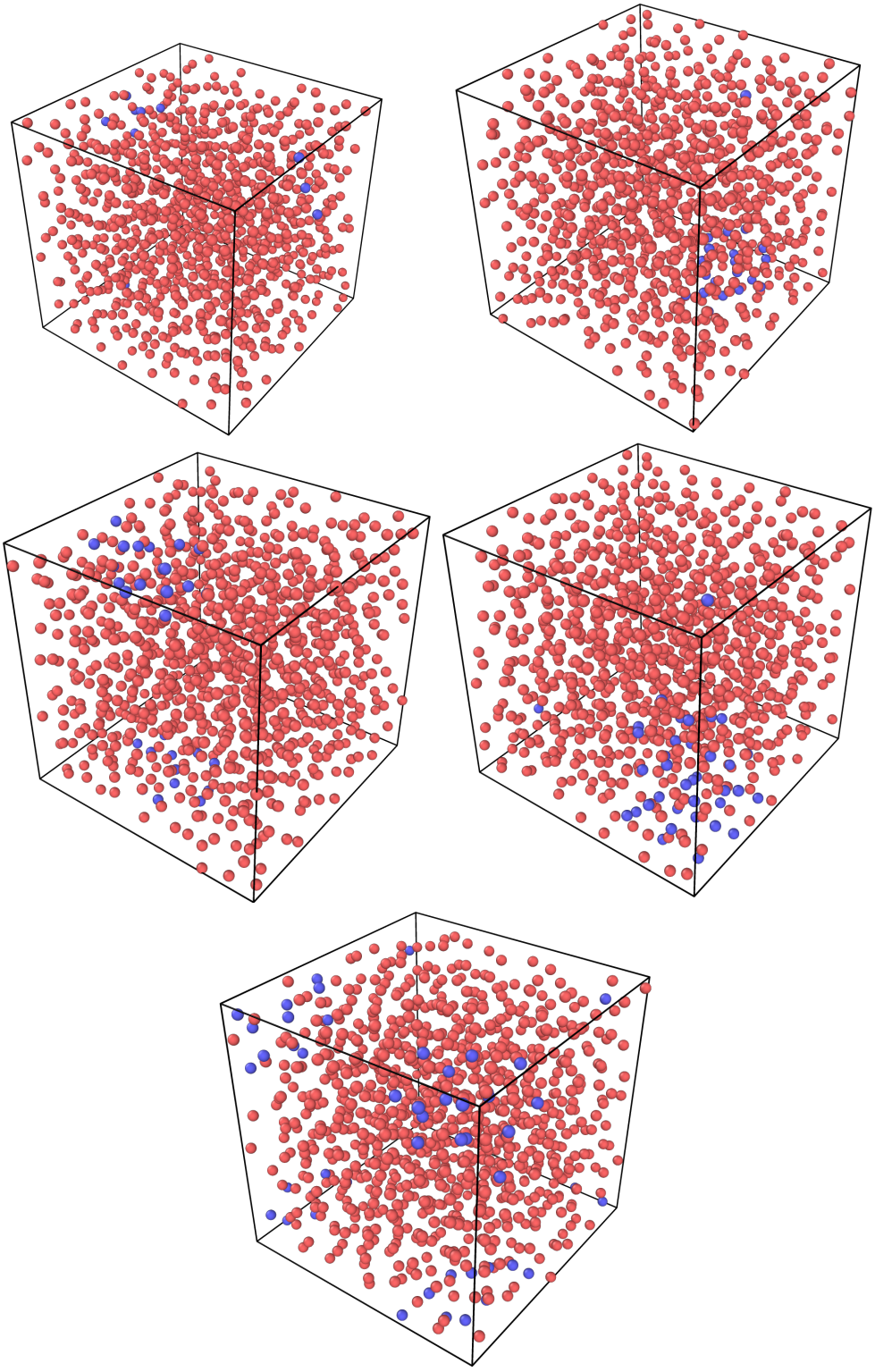

Figure 17: Simulation snapshots from $x = 1\%$ to $x = 5\%$ at $P^* = 0.70$ and $T^* = 0.12$.

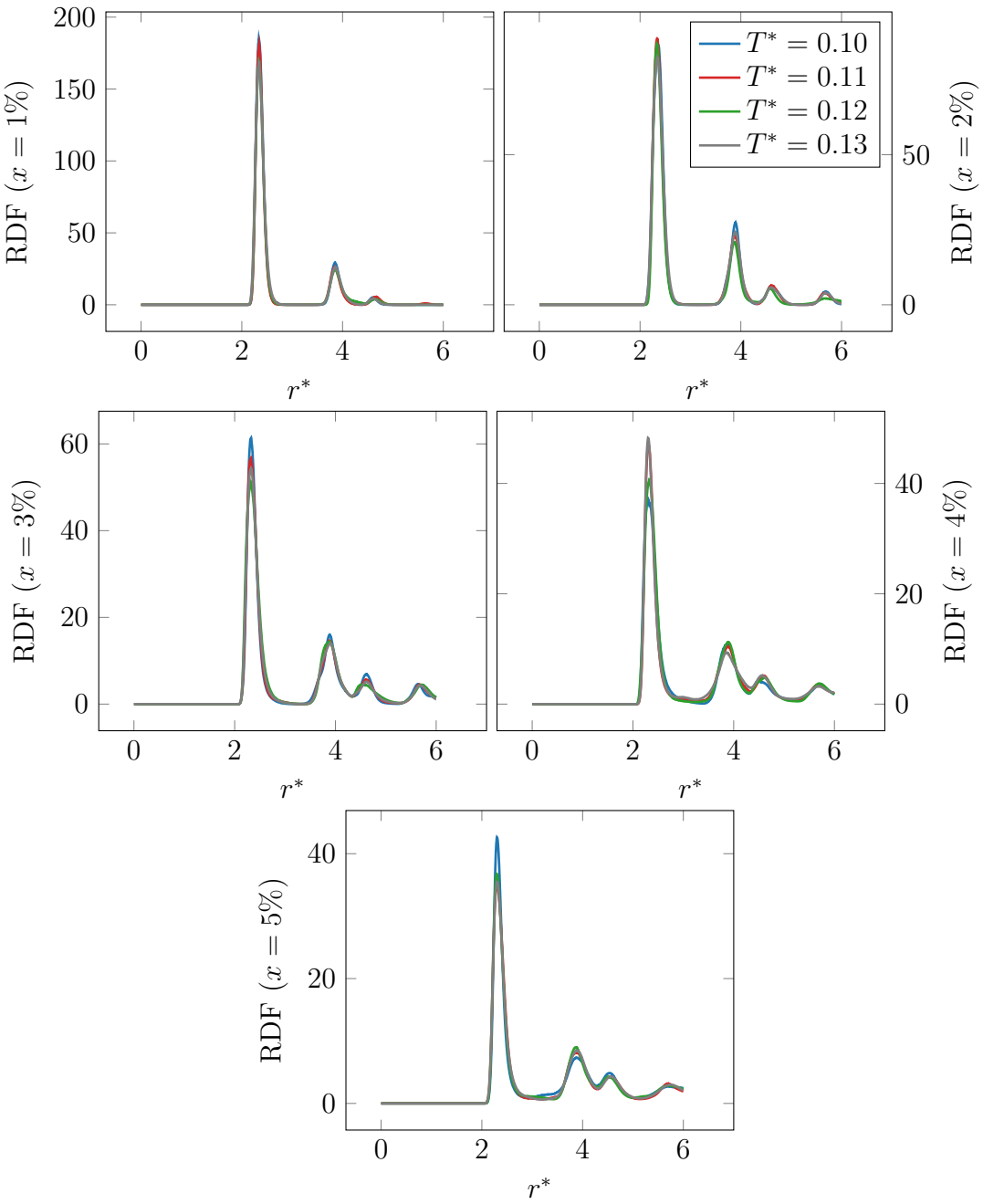

Figure 18: Solute-solute Radial Distribution Function of $P^* = 0.70$ for different concentrations.

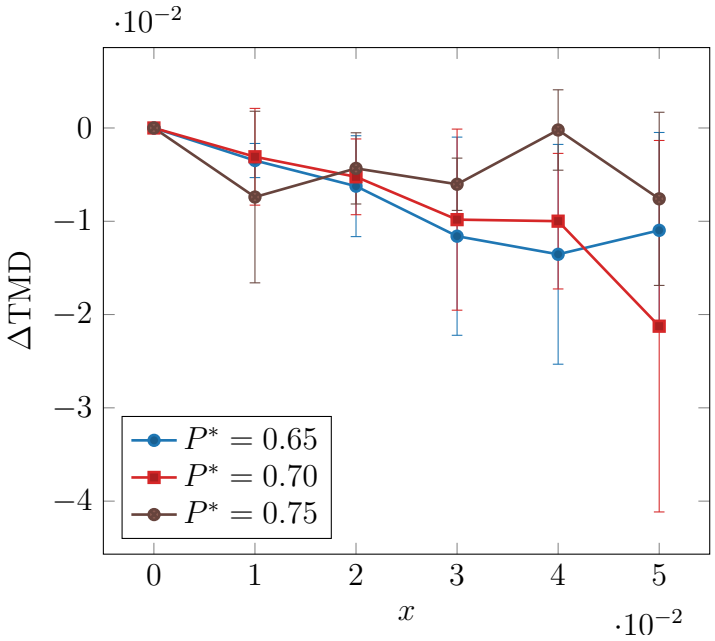

Figure 19: Simulated ΔTMD.

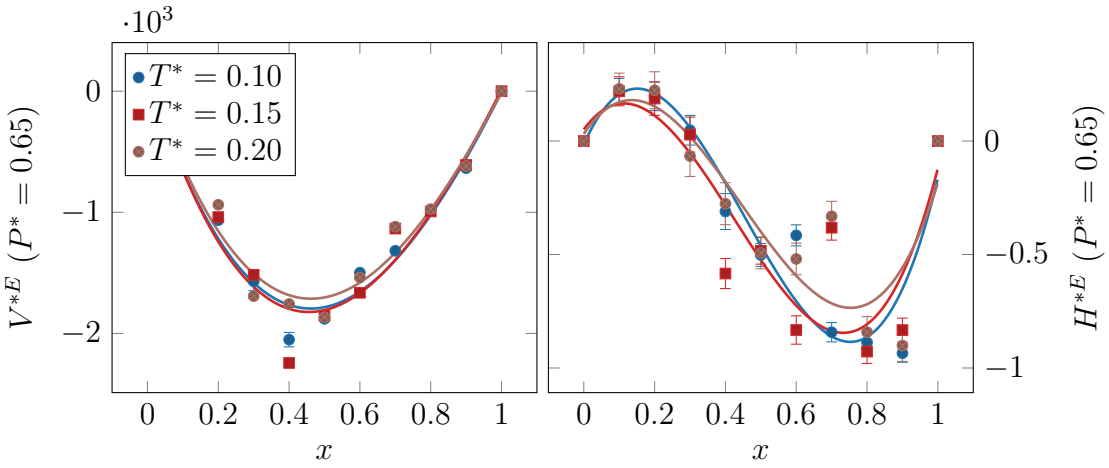

Figure 20: Simulated excess quantities ($P^* = 0.65$). Continuous line is a third-degree polynomial fit.

4 Conclusions

In this work, we studied a one-dimensional model of mixtures. For the solvent-solvent and solvent-solute interactions, we employed a core-softened potential while for the solute-solute we use a one-length scale potential. In a random mixing approximation, when there is no internal structure, we were not able to find a potential that increases the TMD. Exploring the excess quantities we found out that, with this model, they are always symmetric curves for any potential parameters.

Exploring different energy and length parameters in the 1d exact solution, we were able to show that there are potential parameters that, with the addition of solute increases the temperature of maximum density in the high dilution regime. In this solution, the excess functions appear to be symmetric too, with a maximum at $x = 0.5$.

From these sets of parameters which generate an increase in the TMD, we developed a smoothened version of the potential, since the discontinuous version does not present a density anomaly in three dimensions. With this modified potential, we ran Molecular Dynamics simulations and analyzed the behavior of the temperature of maximum density. Analyzing the structure through the RDF, we found out that the solute formed clusters. The excess volume has the same concavity as in the 1D case, while the excess enthalpy shifts from positive to negative values. We verified that, in the 3D version, the TMD decreases for all tested pressures. Thus, for a solvent-solvent and solvent-solute core softened interactions, while in 1 dimension the solute is a structure-maker, in 3 dimensions the solute acts as a structure-breaker. These conclusions were derived from one specific set of parameters. To confirm their universality, this must be evaluated for other sets of parameters.

References

[1] H. Kanno and C. A. Angell. Water: Anomalous compressibilities to 1.9 kbar and correlation with supercooling limits. *The Journal of Chemical Physics*, 70(9):4008–4016, May 1979. doi:10.1063/1.438021.

[2] C. A. Angell, E. D. Finch, and P. Bach. Spin–echo diffusion coefficients of water. *The Journal of Chemical Physics*, 65(8):3063–3066, October 1976. doi:10.1063/1.433518.

[3] F. X. Prielmeier, E. W. Lang, R. J. Speedy, et al. Diffusion in supercooled water to 300 MPa. *Physical Review Letters*, 59(10):1128–1131, September 1987. doi:10.1103/PhysRevLett.59.1128.

[4] F. Franks. *Water: A Matrix of Life*. Royal Society of Chemistry, 2000. ISBN 9780854045839.

[5] P. Debenedetti. *Metastable Liquids: Concepts and Principles*. Physical Chemistry: Science and Engineering. Princeton University Press, 1996. ISBN 9780691085951.

[6] H. J. C. Berendsen, J. R. Grigera, and T. P. Straatsma. The missing term in effective pair potentials. *The Journal of Physical Chemistry*, 91(24):6269–6271, November 1987. doi:10.1021/j100308a038.

[7] J. L. F. Abascal and C. Vega. A general purpose model for the condensed phases of water: TIP4P/2005. *The Journal of Chemical Physics*, 123(23):234505, December 2005. doi:10.1063/1.2121687.

[8] M. W. Mahoney and W. L. Jorgensen. A five-site model for liquid water and the reproduction of the density anomaly by rigid, nonpolarizable potential functions. *The Journal of Chemical Physics*, 112(20):8910–8922, May 2000. doi:10.1063/1.481505.

[9] J. Russo and H. Tanaka. Understanding water's anomalies with locally favoured structures. *Nature Communications*, 5(1):3556, May 2014. doi:10.1038/ncomms4556.

[10] V. Holten, J. C. Palmer, P. H. Poole, et al. Two-state thermodynamics of the ST2 model for supercooled water. *The Journal of Chemical Physics*, 140(10):104502, March 2014. doi:10.1063/1.4867287.

[11] C. Vega, J. L. F. Abascal, M. M. Conde, et al. What ice can teach us about water interactions: a critical comparison of the performance of different water models. *Faraday Discuss.*, 141:251–276, 2009. doi:10.1039/b805531a.

[12] A. de Oliveira, G. Franzese, P. Netz, et al. Waterlike hierarchy of anomalies in a continuous spherical shouldered potential. *The Journal of Chemical Physics*, 128(6): 064901, February 2008. doi:10.1063/1.2830706.

[13] P. Hemmer and G. Stell. Fluids with several phase transitions. *Phys. Rev. Lett.*, 24: 1284–1287, June 1970. doi:10.1103/PhysRevLett.24.1284.

[14] G. Stell and P. Hemmer. Phase transitions due to softness of the potential core. *The Journal of Chemical Physics*, 56(9):4274–4286, 1972. doi:10.1063/1.1677857.

[15] M. Chaplin. Hydrogen bonding in water. `http://lsbu.ac.uk/water/water_hydrogen_bonding.html`, 2020. Last Accessed December 02, 2020. A copy of this page is also available from the Wayback Machine.

[16] P. Debenedetti, V. Raghavan, and S. Borick. Spinodal curve of some supercooled liquids. *The Journal of Physical Chemistry*, 95(11):4540–4551, May 1991. doi:10.1021/j100164a066.

[17] A. Barros de Oliveira, P. Netz, T. Colla, et al. Thermodynamic and dynamic anomalies for a three-dimensional isotropic core-softened potential. *The Journal of Chemical Physics*, 124(8):084505, February 2006. doi:10.1063/1.2168458.

[18] C. Huang et al. The inhomogeneous structure of water at ambient conditions. *Proceedings of the National Academy of Sciences*, 106(36):15214–15218, September 2009. doi:10.1073/pnas.0904743106.

[19] A. Soper and M. Ricci. Structures of High-Density and Low-Density Water. *Physical Review Letters*, 84(13):2881–2884, March 2000. doi:10.1103/PhysRevLett.84.2881.

[20] M. Chaplin. Water clustering. `http://lsbu.ac.uk/water/clusters_overview.html`, 2020. Last Accessed December 02, 2020. A copy of this page is also available from the Wayback Machine.

[21] A. Scala, M. Reza Sadr-Lahijany, N. Giovambattista, et al. Waterlike anomalies for core-softened models of fluids: Two-dimensional systems. *Physical Review E*, 63(4): 041202, March 2001. doi:10.1103/PhysRevE.63.041202.

[22] P. H. Poole, F. Sciortino, U. Essmann, et al. Phase behaviour of metastable water. *Nature*, 360(6402):324–328, November 1992. doi:10.1038/360324a0.

[23] E. A. Jagla. Core-softened potentials and the anomalous properties of water. *The Journal of Chemical Physics*, 111(19):8980–8986, November 1999. doi:10.1063/1.480241.

[24] F. Franks and D. J. G. Ives. The structural properties of alcohol–water mixtures. *Q. Rev. Chem. Soc.*, 20(1):1–44, 1966. doi:10.1039/QR9662000001.

[25] D. González-Salgado, K. Zemánková, E. G. Noya, et al. Temperature of maximum density and excess thermodynamics of aqueous mixtures of methanol. *The Journal of Chemical Physics*, 144(18):184505, 2016. doi:10.1063/1.4948611.

[26] G. Wada and S. Umeda. Effects of nonelectrolytes on the temperature of the maximum density of water. I. alcohols. *Bulletin of the Chemical Society of Japan*, 35(4):646–652, 1962. doi:10.1246/bcsj.35.646.

[27] J. McHutchison. The temperature of maximum density of alcohol-water mixtures. *Journal of the Chemical Society*, 129:1898–1899, 1926. doi:10.1039/JR9262901892.

[28] I. Tomaszkiewicz and S. Randzio. Excess enthalpy in the methanol-water system at 278.15, 298.15 and 323.15 K under pressures of 0.1, 20 and 39 MPa. *Thermochimica Acta*, 103(2):291–295, 1986. doi:10.1016/0040-6031(86)85165-6.

[29] R. F. Lama and Benjamin C.-Y. Lu. Excess Thermodynamic Properties of Aqueous Alcohol Solutions. *Journal of Chemical & Engineering Data*, 10(3):216–219, July 1965. doi:10.1021/je60026a003.

[30] J.B. Ott, G.V. Cornett, C.E. Stouffer, et al. Excess enthalpies of (ethanol+water) at 323.15, 333.15, 348.15, and 373.15 K and from 0.4 to 15 MPa. *The Journal of Chemical Thermodynamics*, 18(9):867–875, 1986. doi:10.1016/0021-9614(86)90121-7.

[31] J.B Ott, C.E Stouffer, G. Cornett, et al. Excess enthalpies for (ethanol + water) at 398.15, 423.15, 448.15, and 473.15 K and at pressures of 5 and 15 MPa. Recommendations for choosing (ethanol + water) as an HmE reference mixture. *The Journal of Chemical Thermodynamics*, 19(4):337–348, 1987. doi:10.1016/0021-9614(87)90115-7.

[32] N. Patel and S. Sandler. Excess volumes of the water/methanol, n-heptane/ethyl acetate, n-heptane/n-butyraldehyde, and n-heptane/isobutyraldehyde systems. *Journal of Chemical & Engineering Data*, 30(2):218–222, April 1985. doi:10.1021/je00040a028.

[33] A. Ben-Naim, A. M. Navarro, and J. M. Leal. A Kirkwood–Buff analysis of local properties of solutions. *Physical Chemistry Chemical Physics*, 10(18):2451, 2008. doi:10.1039/b716116f.

[34] C. Visser, G. Perron, and J. Desnoyers. The heat capacities, volumes, and expansibilities of *tert* -butyl alcohol – water mixtures from 6 to 65 °C. *Canadian Journal of Chemistry*, 55(5):856–862, March 1977. doi:10.1139/v77-119.

[35] E. S. Kim and K. N. Marsh. Excess volumes for 2-methyl-2-propanol + water at 5 K intervals from 303.15 to 323.15 K. *Journal of Chemical & Engineering Data*, 33(3): 288–292, July 1988. doi:10.1021/je00053a020.

[36] F. E. Blacet, P. A. Leighton, and E. P. Bartlett. The specific heats of five pure organic liquids and of ethyl alcohol-water mixtures. *The Journal of Physical Chemistry*, 35 (7):1935–1943, July 1931. doi:10.1021/j150325a005.

[37] E. Rizzatti, M. A. Barbosa, and M. C. Barbosa. Core-softened potentials, multiple liquid–liquid critical points, and density anomaly regions: An exact solution. *Frontiers of Physics*, 13(1):136102, 2018. doi:10.1007/s11467-017-0725-3.

[38] M. A. A. Barbosa, E. Salcedo, and M. C. Barbosa. Multiple liquid-liquid critical points and density anomaly in core-softened potentials. *Physical Review E*, 87(3): 032303, March 2013. doi:10.1103/PhysRevE.87.032303.

[39] H. Takahashi. A simple method for treating the statistical mechanics of one-dimensional substances. *Proceedings of the Physico-Mathematical Society of Japan*, 24:60–62, 1942.

[40] I. Prigogine, A. Bellemans, and V. Mathot. *The Molecular Theory of Solutions*. Series in physics. North-Holland Publishing Company, 1957. ISBN 9780598722003.

[41] S. Salinas. *Introduction to Statistical Physics*. Graduate Texts in Contemporary Physics. Springer, 2001. ISBN 9780387951195.

[42] W. Feller. *An Introduction to Probability Theory and Its Applications, Volume 1*. A Wiley publication in mathematical statistics. Wiley, 1968. ISBN 9780471257080.

[43] H.B. Callen. *Thermodynamics and an Introduction to Thermostatistics*. Wiley, 1985. ISBN 9780471862567.

[44] A. Meurer et al. SymPy: symbolic computing in Python. *PeerJ Computer Science*, 3: e103, January 2017. doi:10.7717/peerj-cs.103.

[45] P. Virtanen et al. SciPy 1.0: Fundamental Algorithms for Scientific Computing in Python. *Nature Methods*, 17:261–272, 2020. doi:10.1038/s41592-019-0686-2.

[46] A. Furlan, E. Lomba, and M. C. Barbosa. Temperature of maximum density and excess properties of short-chain alcohol aqueous solutions: A simplified model simulation study. *The Journal of Chemical Physics*, 146(14):144503, 2017. doi:10.1063/1.4979806.

[47] D. Frenkel and B. Smit. *Understanding molecular simulation: from algorithms to applications*. Elsevier Science, 2002. ISBN 9780080519982.

[48] G. Franzese et al. Metastable liquid-liquid phase transition in a single-component system with only one crystal phase and no density anomaly. *Physical Review E*, 66: 051206, 2002. doi:10.1103/PhysRevE.66.051206.

[49] G. Franzese. Differences between discontinuous and continuous soft-core attractive potentials: The appearance of density anomaly. *Journal of Molecular Liquids*, 136: 267–273, 2007. doi:10.1016/j.molliq.2007.08.021.

[50] S. Plimpton. Fast parallel algorithms for short-range Molecular Dynamics. *Journal of Computational Physics*, 117(1):1–19, March 1995. doi:10.1006/jcph.1995.1039.

[51] O. Tange. GNU Parallel - the command-line power tool. *;login: The USENIX Magazine*, 36(1):42–47, Feb 2011. doi:10.5281/zenodo.16303.